2021 43rd Annual International Conference of the
IEEE Engineering in Medicine & Biology Society (EMBC)
Oct 31 - Nov 4, 2021. Virtual Conference

Validation of an aging virtual population for the study of carotid hemodynamics*

Irene Suriani, *Student member, IEEE,* R. Arthur Bouwman, Massimo Mischi, *Member, IEEE,* Kevin D. Lau

***Abstract*— The analysis of carotid ultrasound (US) flow, velocity, and diameter waveforms provides important information about cardiovascular and circulatory health. These can be used to derive clinical indices of atherosclerosis, vascular aging, and hemodynamic status. To derive clinical insight from carotid waveforms, it is essential to understand the relationship of the observed variability in morphology with the underlying hemodynamic status and cardiovascular properties. For this purpose, using a one-dimensional modeling approach, we have developed and validated a virtual population that is able to realistically simulate carotid waveforms of healthy subjects aged between 10 and 80 years old.**

***Clinical Relevance*—Our virtual population of carotid waveforms can support the interpretation of US patient data. It can be used, e.g., to investigate how waveform morphology and derived indices relate to individual arterial and cardiac properties.**

I. Introduction

Carotid ultrasound (US) shows potential as a hemodynamic monitoring tool in perioperative and critical care settings, due to its non-invasiveness, wide availability, low costs, and ease of placement [1]. Clinical parameters (e.g., cardiac output (CO), fluid responsiveness, arterial stiffness) can be extracted from carotid US waveforms and used to inform decision making (e.g., drugs/fluids administration) [2]. Moreover, indices derived from carotid waveforms were shown to be linked to carotid atherosclerosis [3] and vascular aging [4], [5]. However, there is a need to understand the variability in waveform morphology, which is the result of the complex interaction of central hemodynamic variables (e.g. heart rate (HR), stroke volume (SV), left ventricular ejection time (LVET)), and arterial properties (vessel geometry and stiffness, peripheral vascular resistance (PVR) and compliance (PVC)). Such properties are clinically shown to vary, on average, as a function of age. Here this complex interaction is investigated using a one-dimensional (1D) arterial model [6] in which all these factors can be varied. Age-related changes can be used to parametrize these models as a function of age and generate a wide range of virtual subjects. Previously, Willemet et al. [7] and Charlton et al. [8] have developed two widely documented, 1D-modeling-based, virtual populations (VPs) of arterial pulse wave propagation. Willemet's VP was based on a 55-branch elastic vessel model [6], whose HR, SV, PVR, and elastic and muscular arteries' stiffness and diameter were varied according to clinically reported values across different age groups. However, the carotid artery's diameter and stiffness were assumed to vary with age to the same extent as muscular arteries, despite them being, in reality, predominantly elastic. Charlton's VP was based on a more extensive arterial network comprising of 116 branches, including the cerebral arteries and the arteries of the hands, and used a viscoelastic vessel model. Six parameters (HR, SV, LVET, mean arterial pressure (MAP), vessel diameter, and stiffness) were varied as a function of age. In this case, carotid diameters were varied according to a study by Hansen [9] and stiffness was not directly varied, but calculated for each subject from the diastolic radius using an empirical law [10], optimized to fit the carotid to femoral pulse wave velocity.

In this work, we have extended the approach of Willemet et al., focusing on the study of carotid hemodynamics. We generated a VP of healthy subjects parametrized as a function of age (ranging from 10 to 80 years old, in age decades), by varying a total of 12 model parameters. We improved the definition of carotid-specific variations based on a literature survey, from which it emerged that variations observed in real populations are considerably different from those imposed in previous VPs. We validated our VP against real carotid waveforms available in the literature, based on waveform landmarks and on derived clinical indices.

II. Methods

A. The baseline 55-branch model

For our baseline subject, aged 30-40 years old, we chose the same 55-branch 1D model used by Willemet, initially proposed by Alastruey et al. [6], as illustrated in Fig. 1. The model comprises of the 55 larger arteries in the human arterial network, including the left and right common, external, and internal carotid arteries. In the 1D approach, the vascular system is modeled as a collection of interconnected deformable tube segments, linearly tapered, whose material properties depend on a single spatial coordinate along the vessel axis x (axisymmetry is assumed). Luminal area A, mean blood flow velocity U and pressure P depend on x and

*Research supported by eMTIC, NWO

I. Suriani and M. Mischi are with the Electrical Engineering Department, Eindhoven University of Technology, Groene Loper 3, 5612 AE Eindhoven, Netherlands. (e-mail: i.suriani@tue.nl, m.mischi@tue.nl)

R. A. Bouwman is with the Catharina Hospital, Michelangelolaan 2, 5623 EJ, Eindhoven, Netherlands (e-mail: arthur.bouwman@catharinaziekenhuis.nl).

K. D. Lau is with Philips Research, High Tech Campus 34, 5656 AE Eindhoven, Netherlands. (e-mail: kevin.lau@philips.com).

on time t. Conservation of mass (1) and momentum (2) equations are solved for each segment, together with a tube law (3) relating pressure and area, which takes into account vessel elasticity.

$$\begin{cases} \frac{\partial A(x,t)}{\partial t} + \frac{\partial (A(x,t)U(x,t))}{\partial x} = 0, & (1) \\ \frac{\partial U(x,t)}{\partial t} + U(x,t)\frac{\partial U(x,t)}{\partial x} = -\frac{1}{\rho}\frac{\partial P(x,t)}{\partial x} - \frac{22\pi\mu U(x,t)}{\rho A(x,t)}, & (2) \\ P(x,t) = P_d(x) + \frac{\beta(x)}{A_d(x)}\left(\sqrt{A(x,t)} - \sqrt{A_d(x)}\right). & (3) \end{cases}$$

In (3), A_d is the luminal area at diastolic pressure P_d, β is the wall stiffness parameter, and in (2) ρ and μ are, respectively, the blood density and viscosity, assumed to be constant. The parameter β relates to vessel thickness h and Young's modulus E as

$$\beta(x) = \frac{4}{3}\sqrt{\pi}Eh. \quad (4)$$

Blood is assumed an incompressible Newtonian fluid, with density ρ=1,060 kg/m^3, viscosity μ=2 mPa· s, plug-like velocity profile, and no energy losses at bifurcations. At the inlet of the aorta, a realistic flow waveform is prescribed, and at the terminal branches, RCR Windkessel equivalent circuits are connected, to account for PVR, PVC, and reflections. In our work, the governing equations were solved using a Discontinuous Galerkin scheme, and time integration was performed via the explicit second-order Adam-Bashforth method. The Pulse Wave Solver of NEKTAR++, an open-source spectral/hp-element framework, was adapted and used for simulation. Time stepping was performed with a step size of 0.01 ms, in compliance with the Courant-Friedrichs-Lewy limit, and 15 seconds were simulated to ensure convergence (the convergence criterion was for the difference in consecutive peak systolic pressures to be <0.0001 Pa). Arterial waveforms were simulated throughout the network. For this study, we extracted area, velocity, and flow (i.e. instantaneous area times velocity) waveforms at the mid-point of the left common carotid vessel.

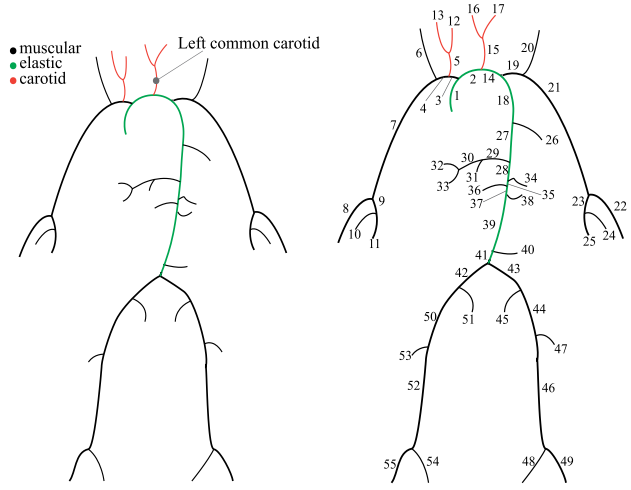

Figure 1. A schematic of the 55-branch baseline model, with different colors for the regions where different age-variations were applied. Left: the point at which we extract the simulated carotid waveforms is indicated. Right: all numbered arteries.

B. Parametrization of the model as a function of age

Aging was simulated by scaling 12 parameters from the baseline model as a function of age. The percentage variations applied are summarized in Table 1. Carotid diameter (D_{car}) and pulse wave velocity (c_{car}) variations were defined by averaging variations reported by 9 different studies [4], [9], [11]–[17], from a total of 3,067 subjects. Variations in c_{car} were based on the reported variations in the stiffness index β, which is related to c [11] as

$$c = \sqrt{\frac{\beta P_s}{2\rho}} \quad (5)$$

where P_s is the systolic pressure. Variations for elastic and muscular arteries followed Willemet et al [7]. Aortic length (L_{ao}), SV, and peripheral vascular compliance (PVC) were varied with age using the linear relations proposed by Charlton et al [8]. PVR variations followed from reported average MAP values across different age groups [18], by considering PVR≈MAP/CO. HR variations were averaged from values reported in two studies[18], [19], and LVET was varied non-linearly with HR according to the formula by Ursino et al.[20].

TABLE I. PERCENTAGE VARIATIONS WITH RESPECT TO BASELINE (30-39 YEARS OLD) APPLIED TO MODEL PARAMETERS PER AGE GROUP. ABBREVIATIONS: D, DIAMETER; C, LOCAL PULSE WAVE VELOCITY; CAR, CAROTID; EL, ELASTIC ARTERY; MUSC, MUSCULAR ARTERY; L, LENGTH; AO, AORTA; HR, HEART RATE; SV, STROKE VOLUME; PVR, PERIPHERAL VASCULAR RESISTANCE; PVC, PERIPHERAL VASCULAR COMPLIANCE, LVET, LEFT VENTRICULAR EJECTION TIME.

Model para-meter	**Variations, % Age group, years**						
	10-19	***20-29***	***30-39***[a]	***40-49***	***50-59***	***60-69***	***70-79***
c_{car}	-16	-6	0	+10	+20	+30	+34
c_{el}	-20	-20	0	+30	+60	+90	+125
c_{musc}	-20	-20	0	0	+15	+15	+30
D_{car}	-10	-6	0	+2	+6	+8	+14
D_{el}	0	0	0	0	+20	+20	+40
D_{musc}	0	0	0	0	+21	+21	+21
L_{ao}	-15	-7	0	7	+15	+22	+30
HR	+11	+5	0	0	0	-2	-4
SV	+8	+4	0	-4	-8	-12	-16
PVR	-22	-13	0	+8	+16	+24	+31
PVC	+26	+13	0	-13	-26	-38	-51
LVET	Varied non-linearly with HR according to Ursino et al. [20]						

a. Baseline age group.

A template aortic flow waveform was scaled to match HR, SV, and LVET variations (Fig. 2), and prescribed at the inlet of the models.

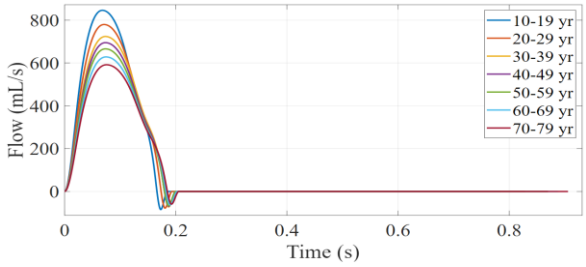

Figure 2. Prescribed aortic flow waveforms per age group.

C. Validation against in-vivo data

We validated our VP against in-vivo studies which reported carotid flow waveforms and derived indices for different age groups. To do so, we implemented a script to automatically

track the amplitude and timings of the waveform landmarks described by Gwilliam et al. [21] on the simulated waveforms (Fig. 5). The landmarks were then used to calculate a set of indices of clinical interest, summarized in Table 2. These were shown to vary with age, in particular: Fsr/Vsr increased significantly, Fed/Ved decreased, and both PI and FAI increased with age [4], [5]. FAI is indicated as a measure of peripheral wave reflection [4], and PI, RI, and FAI are all indicators of presence and stage of carotid atherosclerosis [3].

TABLE II. CAROTID WAVEFORM INDICES

Index[a]	Symbol	Derivation from landmarks[b]
Mean of waveform	F_m, V_m	Mean of all waveform amplitude values
Normalized peak systolic value	F_s, V_s	$P1/F_m$, $P1/V_m$
Normalized secondary peak in systole	F_{sr}, V_{sr}	$P2/F_m$, $P2/V_m$
Normalized end-diastolic value	F_{ed}, V_{ed}	$D4/F_m$, $D4/V_m$
Pulsatility index	PI	$(P1-D4)/F_m$, $(P1-D4)/V_m$
Resistance index	RI	$(P1-D4)/P1$
Flow augmentation index	FAI	$(P2-D4)/(P1-D4)$

a. Calculated either from velocity or flow waveforms
b. See Fig. 5

III. RESULTS

Simulated carotid flow waveforms per age group are shown in Fig. 3.

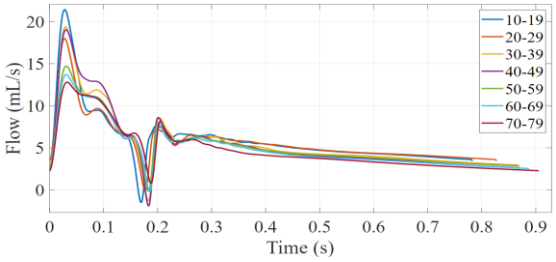

Figure 3. VP carotid flow waveforms.

A. Validation against in-vivo data

Comparison to US-derived values reported by Hirata et al. [4] for three age groups (<40, 40-60, and >60) for all VPs (ours, Willemet's, and Charlton's) is shown in Fig. 4a-b. Furthermore, we compared flow-derived PI to in-vivo values reported by two separate studies based on PC-MRI data: Gwilliam et al. [21], concerning a younger population aged 20-40, and Hoi et al. [5] based on an older cohort aged 40-90. These are shown in Fig. 6.

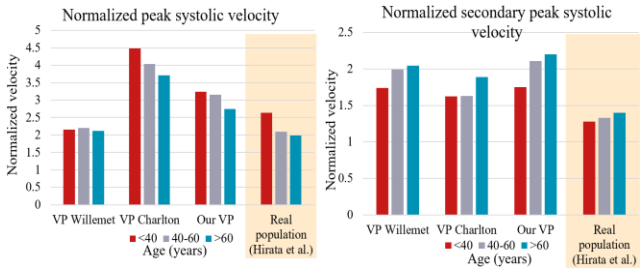

Figure 4-a. Carotid indices (V_s,V_{sr}) of the three VPs compared to reference values.

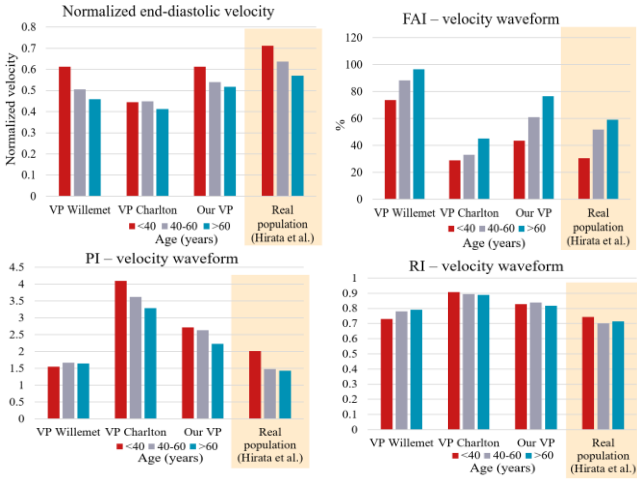

Figure 4-b. Carotid indices (V_{ed}, FAI, PI, RI) of the three VPs compared to reference values.

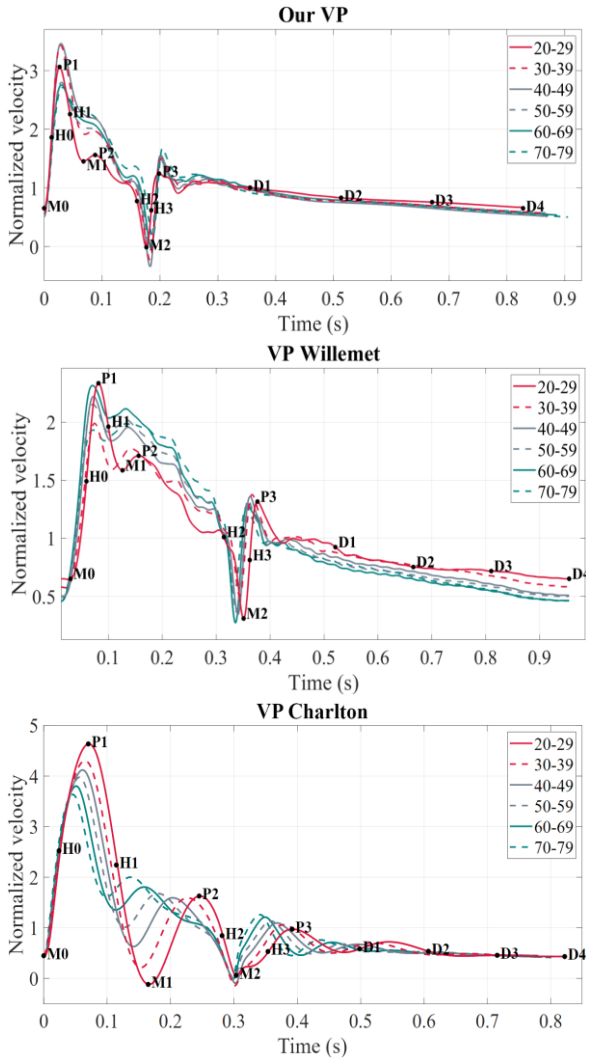

Figure 5. Carotid waveform landmarks identified on the three VPs. Waveforms pertaining to each of the three age groups considered are colored in reference to Fig.4: magenta for <40, grey for 40-60, teal for >60. Waveforms normalized by V_m, in order to facilitate comparison.

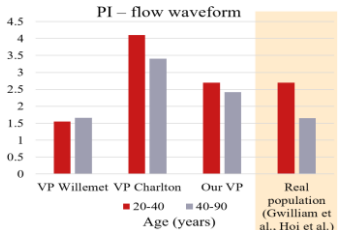

Figure 6. PI indices of the three VPs compared to PI values of two real populations.

IV. Discussion

For several of the clinical indices considered, our VP better reflects the trends and value ranges observed by Hirata [4] in a real population: particularly V_s, FAI, and PI. Moreover, amongst the three VPs, ours was the only one to reflect the correct trends in all indices (except for RI, for which no age-related trend was observed in the real population). Also, when considering flow-derived PI, validated against two PC-MRI-based studies [5], [21], our VP best reflects the real population both in trend and absolute values. Our VP is based on an improved definition of specific age-related variations in c_{car} and D_{car}. This is shown in Fig. 7, containing a comparison between the average variations reported in the literature, which we imposed in our VP, and the ones imposed in the previous VPs. Charlton's variations were derived using the supplemental online material available at the address provided in the endnote of [8]. A limitation of this study is that our VP was based on a simplified arterial model, which assumes a uniform velocity profile across all vessels (which might be inaccurate especially at peripheral sites) and neglects the viscous properties of arterial walls.

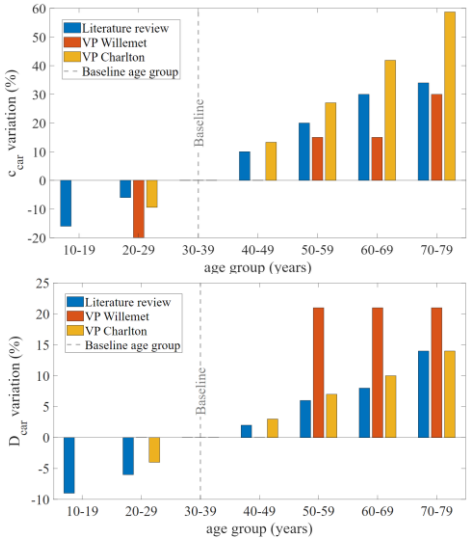

Figure 7. Literature age-variations in c_{car} and D_{car} vs the ones imposed in previous VPs.

V. Conclusion

We developed a VP of subjects aged between 10 and 80 years old. Age-dependent carotid-specific variations were based on novel literature-based values. The VP showed characteristics comparable to real carotid waveforms reported in the literature. The VP can be used to investigate the impact of arterial and cardiac properties on carotid waveform morphology (quantified by the defined landmarks' amplitude and timings) and derived indices. It can also be used to test waveform analysis algorithms across virtual subjects of different ages.

References

[1] M. Gassner, *et al.*, "Feasibility of common carotid artery point of care ultrasound in cardiac output measurements compared to invasive methods," J. Ultrasound, 18, 2, 127–133, 2015.

[2] L. Beier, *et al.*, "Carotid Ultrasound to Predict Fluid Responsiveness," J. Ultrasound Med., 39, 10, 1965–1976, 2020.

[3] M. Rafati, *et al.*, "Appraisal of different ultrasonography indices in patients with carotid artery atherosclerosis," EXCLI J., 16, 727–741, 2017.

[4] K. Hirata, *et al.*, "Age-related changes in carotid artery flow and pressure pulses: Possible implications for cerebral microvascular disease," Stroke, 37, 10, 2552–2556, 2006.

[5] Y. Hoi, *et al.*, "Characterization of volumetric flow rate waveforms at the carotid bifurcations of older adults," Physiol. Meas., 31, 3, 291–302, 2011.

[6] J. Alastruey, *et al.*, "Arterial pulse wave haemodynamics," In S. Anderson (Ed.), 11th Int. Conf. on Pressure Surges, 2012.

[7] M. Willemet, *et al.*, "A database of virtual healthy subjects to assess the accuracy of foot-to-foot pulse wave velocities for estimation of aortic stiffness," Am. J. Physiol. Heart. Circ. Physiol., 663–675, 2015.

[8] P. H. Charlton, *et al.*, "Modeling arterial pulse waves in healthy aging: a database for in silico evaluation of hemodynamics and pulse wave indexes," Am. J. Physiol. Heart Circ. Physiol., 317, 5, H1062–H1085, 2019.

[9] F. Hansen, *et al.*, "Diameter and compliance in the human common carotid artery - variations with age and sex," Ultrasound Med. Biol., 21, 1, 1–9, 1995.

[10] J. P. Mynard and J. J. Smolich, "One-Dimensional Haemodynamic Modeling and Wave Dynamics in the Entire Adult Circulation," Ann. Biomed. Eng., 43, 6, 1443–1460, 2015.

[11] T. Uejima, *et al.*, "Age-specific reference values for carotid arterial stiffness estimated by ultrasonic wall tracking," J. Hum. Hypertens., 34, 214–222, 2020.

[12] R. S. Reneman, *et al.*, "Age-related changes in carotid artery wall properties in men," Ultrasound Med. Biol., 12, 6, 465–471, 1986.

[13] A. Benetos, *et al.*, "Arterial alterations with aging and high blood pressure. A noninvasive study of carotid and femoral arteries," Arterioscler. Thromb. Vasc. Biol., 13, 1, 90–97, 1993.

[14] Å. R. Ahlgren, *et al.*, "Stiffness and diameter of the common carotid artery and abdominal aorta in women," Ultrasound Med. Biol., 23, 7, 983–988, 1997.

[15] C. Sass, *et al.*, "Intima-media thickness and diameter of carotid and femoral arteries in children, adolescents and adults from the Stanislas cohort: Effect of age, sex, anthropometry and blood pressure," J. Hypertens., 16, 11, 1593–1602, 1998.

[16] L. A. Bortolotto, *et al.*, "The aging process modifies the distensibility of elastic but not muscular arteries," Hypertension, 34, 4 II, 889–892, 1999.

[17] J. Joseph, *et al.*, "Carotid Stiffness Variations in the Presence of Established Risk Factors: Observations from a Clinical Study Using ARTSENS," IEEE Med. Meas. Appl. MeMeA 2020 - Conf. Proc., 2020.

[18] C. M. McEniery, *et al.*, "Normal vascular aging: Differential effects on wave reflection and aortic pulse wave velocity - The Anglo-Cardiff Collaborative Trial (ACCT)," J. Am. Coll. Cardiol., 46, 9, 1753–1760, 2005.

[19] A. I. Yashin, *et al.*, "Insights on aging and exceptional longevity from longitudinal data: Novel findings from the Framingham heart study," Age (Omaha), 28, 4, 363–374, 2006.

[20] M. Ursino, "Interaction between carotid baroregulation and the pulsating heart: A mathematical model," Am. J. Physiol. Hear. Circ. Physiol., 275, 5, 44-5, 1733–1747, 1998.

[21] M. N. Gwilliam, *et al.*, "MR derived volumetric flow rate waveforms at locations within the common carotid, internal carotid, and basilar arteries," J. Cereb. Blood Flow Metab., 29, 12, 1975–1982, 2009.